water

MDPI

Article

Flood Evacuation Routes Based on Spatiotemporal Inundation Risk Assessment

Yoon Ha Lee [1], Hyun Il Kim [2], Kun Yeun Han [2] and Won Hwa Hong [3,*]

[1] Sustainable Building Material and Construction Laboratory, Hanyang University, Erica Campus, 55 Hanyangdaehak-ro, Sangnok-gu, Ansan, Gyeonggi-do 15588, Korea; dldbsgk123@naver.com
[2] Department of Civil Engineering, Kyungpook National University, 80 Daehak-ro, Buk-gu Daegu 41566, Korea; hyuun228@gmail.com (H.I.K.); kshanj@knu.ac.kr (K.Y.H.)
[3] School of Architectural, Civil, Environmental and Energy Engineering, Kyungpook National University, 80 Daehak-ro, Buk-gu Daegu 41566, Korea
* Correspondence: hongwonhwa@gmail.com; Tel.: +82-53-950-5597

Received: 23 July 2020; Accepted: 11 August 2020; Published: 13 August 2020

check for updates

Abstract: For flood risk assessment, it is necessary to quantify the uncertainty of spatiotemporal changes in floods by analyzing space and time simultaneously. This study designed and tested a methodology for the designation of evacuation routes that takes into account spatial and temporal inundation and tested the methodology by applying it to a flood-prone area of Seoul, Korea. For flood prediction, the non-linear auto-regressive with exogenous inputs neural network was utilized, and the geographic information system was utilized to classify evacuations by walking hazard level as well as to designate evacuation routes. The results of this study show that the artificial neural network can be used to shorten the flood prediction process. The results demonstrate that adaptability and safety have to be ensured in a flood by planning the evacuation route in a flexible manner based on the occurrence of, and change in, evacuation possibilities according to walking hazard regions.

Keywords: spatiotemporal flood fluctuations; inundation risk assessment; evacuation route; artificial neural network; geographic information system

1. Introduction

Natural disasters threaten the lives and valuable assets of thousands of people every year [1], and widespread destruction, economic loss, and loss of life are global phenomena. Korea is historically vulnerable to flooding due to high precipitation (annual precipitation in Seoul is 1200–1600 mm) compared to other regions of the same latitude [2]. Generally, flooding is caused by a complex combination of meteorological and hydrological phenomena such as extreme rainfall and flowing water [3]. Moreover, an impermeable layer such as a road or paved surface in an urban development assigns much more vulnerability to any given rainfall runoff phenomenon. Losses due to flooding can be reduced by better land-use planning, regulations, law enforcement, and non-physical mitigation management such as the establishment of shelters and evacuation routes [4]. Disaster managers are attempting to predict floods and flood management and establish action plans by utilizing prediction materials. The main purpose of flood prediction is to eliminate or lessen the causal factors that trigger flood disasters [5]. For example, successful prediction of rainfall and flood progress is utilized in flood management by such means as the preparation of flood hazard maps, contributing significantly to the reduction of casualties [6]. Representative models for predicting urban flooding include deterministic models based on numerical analysis and data-driven models using artificial neural networks that have learned the rainfall runoff relation. In the case of urban flooding prediction based on a numerical analysis model, this provides accurate and precise results, but the problem is that pre- and post-processing takes quite some time. In the case of data-driven models, one possibility is to employ a stochastic model that is based on data established in advance, including target values and real-time simulation or prediction using an artificial neural network (ANN). In particular, if the database used in a data-driven model is based on the result of deterministic model results, it carries the advantage of enhancing the accuracy of the target value's representation while simultaneously securing sufficient time for evacuation [7].

To date, studies using artificial neural networks, genetic algorithms, and deep learning models have been carried out variously with the purpose of predicting or controlling floods. According to Mosavi et al. [8], the application of machine learning to hydraulic and hydrology has increased. According to the same study, there is no absolutely predominant machine learning model, and it seems that useful machine learning techniques differ depending on the purpose, data, and results of the study. Jhong et al. [9] established an inundation prediction model by combining support vector machine (SVM) and multi-objective genetic algorithm (MOGA) based on effective materials concerning typhoons, and this made it possible to reduce the prediction time and to optimize input data. Granata et al. [10] conducted post-rainfall overflow analysis through support vector regression (SVR) and compared it with the results of the US Environmental Protection Agency's Storm Water Management Model (EAP-SWMM) to demonstrate that overflow had been overestimated in comparison to the SVR results. Tehrany et al. [11] used the SVR to analyze flood susceptibility with different kinds of kernel function. This research indicated that SVR could yield reliable assessment results for a flood susceptibility map. Chang et al. [12] predicted flood depth, enabling sufficient time for evacuation by using rainfall and stream runoff data and comparison with simulation results that indicated outstanding prediction capability. A prediction of stream runoff was carried out by Zhou et al. [13], using the radial basis function network (RBFN), extreme learning machine (ELM), and Elman network's ensemble technique. Empirical wavelet transform (EWT) was employed for data pre-processing, and the average monthly runoff of the stream subject to study was predicted. Deep learning techniques have been adopted in the water resource field to enhance floodgate predictions and to include more concepts in the model. Hu et al. [14] used long short-term memory (LSTM) for rainfall runoff simulation with 86 items of rainfall runoff pattern data. These results were compared with the ANN model to validate the superiority of the LSTM neural network. Rahman et al. [15] developed a method by integrating artificial neural network (ANN), logistic regression (LR), frequency ratio (FR), and analytical hierarchy process (AHP) for flood susceptibility assessment. The integrated LR-FR model showed high predictive power. This series of studies opens up new opportunities for planning and designing flood control measures.

Meanwhile, evacuation is an effective measure for minimizing damage and loss of life caused by flooding [16,17]. However, according to studies on the lessons that can be learned from disasters, it is apparent that, sometimes, evacuation to designated evacuation centers is not carried out [18–20]. The reasons for this were diverse and included problems in forecast and warning systems, in the location of evacuation centers and evacuation routes, and in evacuation center functions. Such studies throw doubt on the practicality of flood management policies, such as the preparation of evacuation maps based on maximum inundation scope and flood depth. Meanwhile, the problem of assigning location can be defined according to two factors—space and time—and, fundamentally, these two factors must be analyzed simultaneously [21]. In addition, the impacts of spatial and temporal changes in flooding can have significant consequences for the assessment of urban flood risks [22]. From this perspective, a few studies have recently conducted spatial and temporal analyses of urban flooding. Huang et al. [23] analyzed the spatial–temporal patterns of urban floods during the period of 2009–2015 in the central area of Guangzhou, China. Ahmad and Simonovic [22] mentioned that although it is necessary to quantify the uncertainty of spatial and temporal changes in flood inundation, this was hardly considered. Furthermore, they developed a map demonstrating the spatial and temporal variation in reliability vulnerability, robustness, and resiliency indices through fuzzy analysis. Chen et al. [24] integrated the flood risk factors for coastal lowland regions in 1970, 2004, and 2013 using a geographic information system (GIS) and analyzed flood hazard assessment maps for each of those years based on multi-criteria decision analysis. Results demonstrated that flood occurrence was extremely variable in terms of time and space, depending on the associated flood risk factors. Therefore, considering such circumstances in general, the appropriate solution to the problem of evacuation route assignment should consist of real-time evacuation guidance following temporal and spatial inundation progress. This study aimed to propose a methodology for designating such real-time evacuation route guidance by analyzing spatial inundation progress following temporal inundation progress. We aimed to predict flood overflow using a dynamic artificial neural network and to analyze expected flood regions in advance through a two-dimensional submergence analysis of city regions. A methodology then was proposed for designating an evacuation route based on inundation progress and evacuation by walking hazard, and this was applied to the study area.

2. Materials and Methods

This study aimed to propose and apply a method for designating evacuation routes following temporal and spatial inundation progress due to doubt in the practicality and utilization of the method of preparing evacuation maps based on maximum inundation scope and flood depth.

The study comprised two stages, and the study flow can be seen in Figure 1 below.

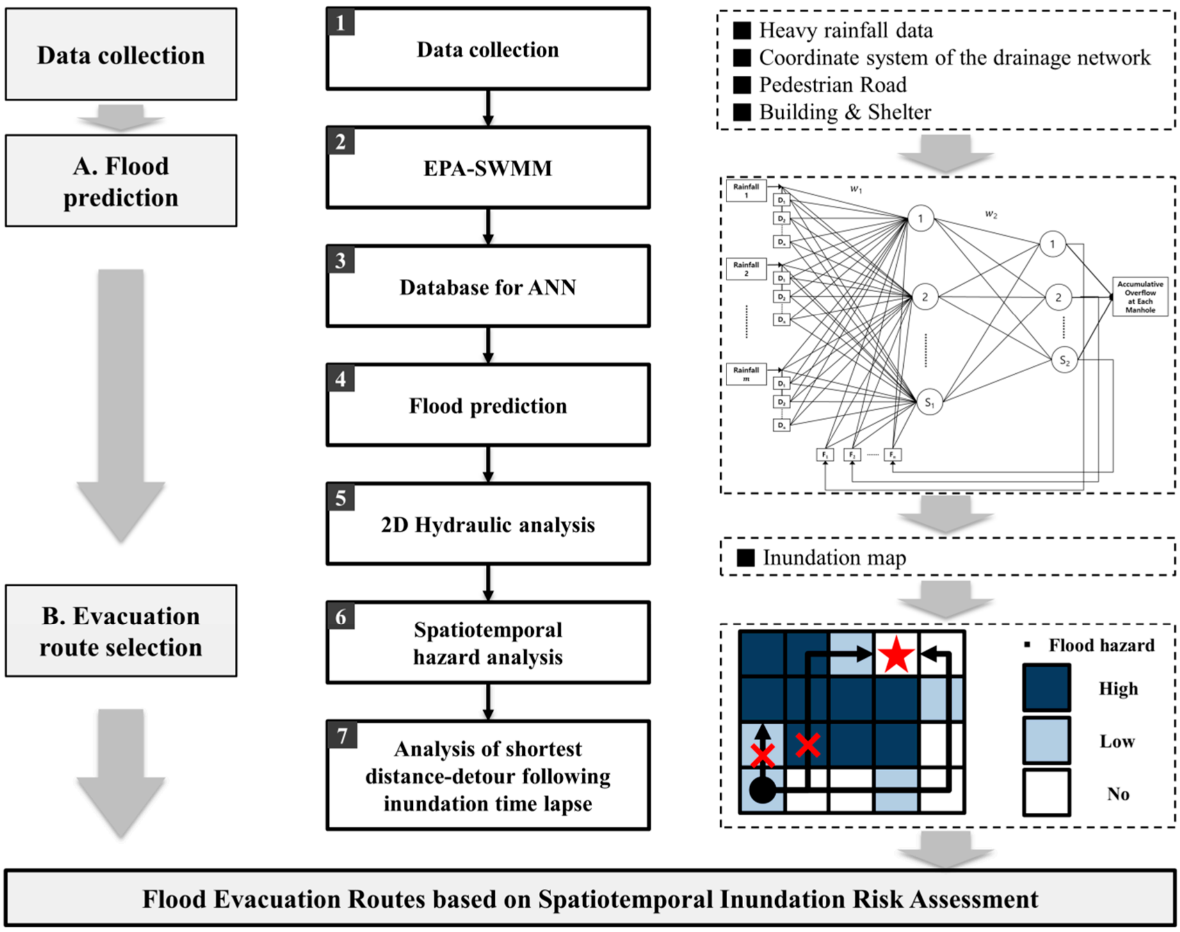

Figure 1. Flowchart of study methodology.

The first stage consisted of executing an inundation prediction for the study area. For this purpose, various rainfall scenarios were analyzed and a one-dimensional runoff interpretation was carried out with the SWMM provided by the EPA. SWMM is a one-dimensional urban runoff model based on hydraulic calculation with consideration of the drainage network system. In this study, SWMM was used to calculate the overflows in the urban basin, which were used as target data of the NARX

(Nonlinear Auto Regressive with eXogenous inputs) neural network. Accordingly, dynamic neural network input and learning were executed based on the accumulative rainfall–accumulative outflow and established so as to enable the prediction of accumulative overflow in real-time for specific rainfall instances. In this study, data concerning rainfall in the Gangnam region (Seoul city, Korea) which lasted for 6 h on 21 September 2010 were used and the accumulative overflow was predicted. A two-dimensional flood analysis was conducted based on predicted accumulative overflow and, in turn, the flood depth and velocity of flow were calculated for every 10 min period during this 2010 occurrence of heavy rain in the study area.

The second stage involved the prediction of a safe evacuation route in consideration of spatial and temporal demand change. Inundation scope by duration, flood depth, and flow velocity were utilized to assign a flood hazard grade for inundation scope, using the risk calculation method proposed by the UK Department for Environment, Food and Rural Affairs (DEFRA) and the Environment Agency [25]. The flood hazard grade classified the evacuation by walking possibility per duration by overlapping with the pedestrian road network within the study area. In addition, a methodology for identifying the shortest route from buildings within the expected flood region to the designated evacuation center, or a detour route, was proposed.

The materials utilized for the methodology for the evacuation route prediction proposed in this study are shown in Table 1 below.

Table 1. Required data.

Objective	Data	Properties	Data Collection Source
A. Flood prediction	Rainfall scenario	Rainfall data in 10 min units, duration	Calculation of probable rainfall and Meteorological Administration Agency data
	Overflow per manhole point	Overflow, duration of velocity of flow	SWMM interpretation result
	Predicted accumulative overflow	Accumulative overflow, duration of velocity of flow	Prediction result of NARX neural network
	Digital elevation map (DEM)	Grid coordinates and elevation	LiDAR detailed topographic map
B. Evacuation route selection	Building	Coordinates, purpose	www.juso.go.kr
	Evacuation shelter	Coordinates, area	https://safecity.seoul.go.kr
	Pedestrian road data	Coordinates	www.juso.go.kr
	Predicted flood data	Maximum and hourly flood depth per grid	Comprehensive analysis results of NARX and 2D immersion analysis program

3. Results

3.1. Study Area

In this study, the drainage sectors of Nonhyeon, Yeoksam, Seocho-3, Seocho-4, and Seocho-5, including the Gangnam station region, were selected as the study area. The total area of the study area was 7.4 km^2 and the areas of each drainage sector were 1.8 km^2 for Nonhyeon, 1.9 km^2 for Yeoksam, 1.8 km^2 for Seocho-3, 1.1 km^2 for Seocho-4, and 0.8 km^2 for Seocho-5 (Figure 2).

The study area, that is, the Gangnam station area, is relatively low in comparison with the other regions, and with its complex sewer network, it can be considered a place with a high inundation risk [26]. Moreover, it has a history of inundation in excess of 1.4 km^2 as evidenced by an inundation trace tap caused by heavy rainfall on 21 September 2010. The major manhole points selected in this study, taking account of the SWMM, overflow, and frequency, are depicted in Figure 3.

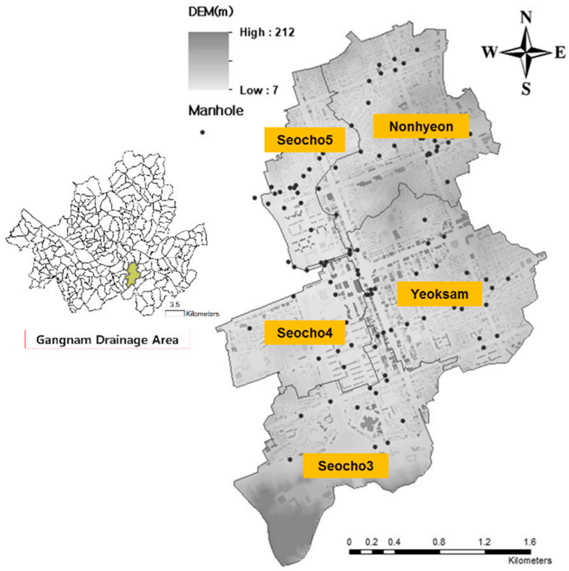

Figure 2. Study area: Gangnam drainage area, Seoul metropolitan city, Korea.

Figure 3. Establishment of Storm Water Management Model (SWMM) and major manhole points.

3.2. Artificial Neural Network-Based Inundation Forecasting

In this study, the flood overflow prediction model was established for the subject regions with sufficient lead time in order to provide two-dimensional inundation mapping for calculating the evacuation center location and evacuation route by hour. The NARX was used as the neural network. NARX is a circulation-type dynamic neural network with a feedback connection surrounding multiple neural network layers and has high learning ability for times series-based input data [27]. In this study, the NARX neural network consisted of an input layer, one hidden layer, and a layer for output. A single hidden layer neural network was used because there was insufficient data to use more than two hidden layers. The input layer contains rainfall input data and feedback target data.

The input rainfall data for NARX used 24 probability rainfalls with a duration of 1 h, 80 probability rainfalls with a duration of 2 and 3 h, and 18 observed rainfalls. The 24 sets of probability rainfall data correspond to durations of 1 h in 10 mm increments of rainfall, ranging from 50 mm to 100 mm in total. In addition, for rainfall, a rainfall duration of 2 or 3 h and a total of 80 rainfall events were used with Huff's temporal distribution data on rainfall frequencies of 2, 3, 5, 10, 20, 30, 50, 70, 80, and 100 year periods. Each accumulated rainfall event was made from a single sequence of data (Figure 4a). The target value data was used by accumulating SWMM simulation results for each rainfall event and making them into a single sequence of data (Figure 4b). Following this, the input value and target value of the neural network can be seen in Figure 4. The exogenous input for NARX training is accumulative overflow in this study. A total of 103 manholes were considered and over 122 scenarios, actual rainfall event data, and accumulative overflow data for each manhole were used for learning. Data for training, validation, and testing were used by randomly extracting 70%, 15%, and 15% from all data. To avoid overfitting, all of the aforementioned 122 rainfall runoff data sets were applied to NARX, and the datasets for training, validation, and testing were chosen randomly. The prediction of accumulative overflow for each manhole point was conducted for the 21 September 2010 rainfall.

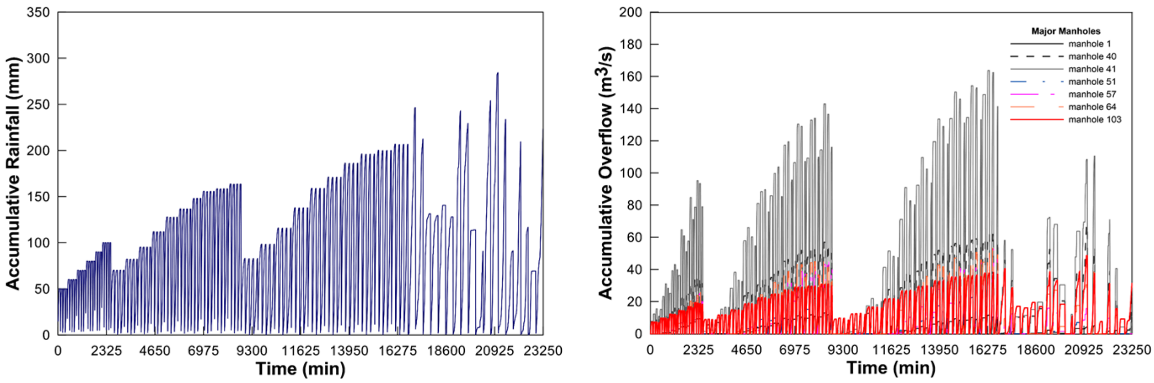

(**a**) (**b**)

Figure 4. Flood prediction training data: (**a**) input data; (**b**) target data.

The NARX neural network has two main parameters; one is the delay time of input data (p) and the other is the delay time of target (feedback) data (q). In this study, the values of 1, 3, and 6 were applied to q parameter, and the value of 0 was used for p parameter. As the time delay of target data increased, the number of feedback input data was more plentiful. The accumulative overflow prediction by manhole point for the study region was conducted with prediction time delays of T + 1 (10 min), T + 3 (30 min), and T + 6 (60 min). The prediction time delay could be selected by the user. It was performed to confirm the prediction result of NARX according to the time delay. When using the T + 1 delay time, two target value data were fed back to the input layer, and when using the T + 3 delay time, four target value data were fed back to the input layer. When using T + 6 delay time, six target value data were fed back to the input layer. As the number of feedback data increased, the learning time increased. With regard to the 2010 rainfall event subject to prediction, the SMWW result was calculated at seven manhole points, and the NARX prediction was also made for seven manhole points (Figure 5).

The results from the NARX neural network were evaluated together with statistical analysis of the previously constructed input data. The performance was evaluated using the root mean square error (RMSE) to compare the SWMM results with prediction model results as a basic index, as defined in Equation (1). The RMSE is an index that quantifies the error between the simulation value and prediction result. The RMSE at each manhole is shown in Table 2.

$$\mathrm{RMSE} = \sqrt{\frac{\sum \left(\mathrm{Q}_{\mathrm{simulated}} - \mathrm{Q}_{\mathrm{predicted}}\right)^2}{\mathrm{n}}} \quad (1)$$

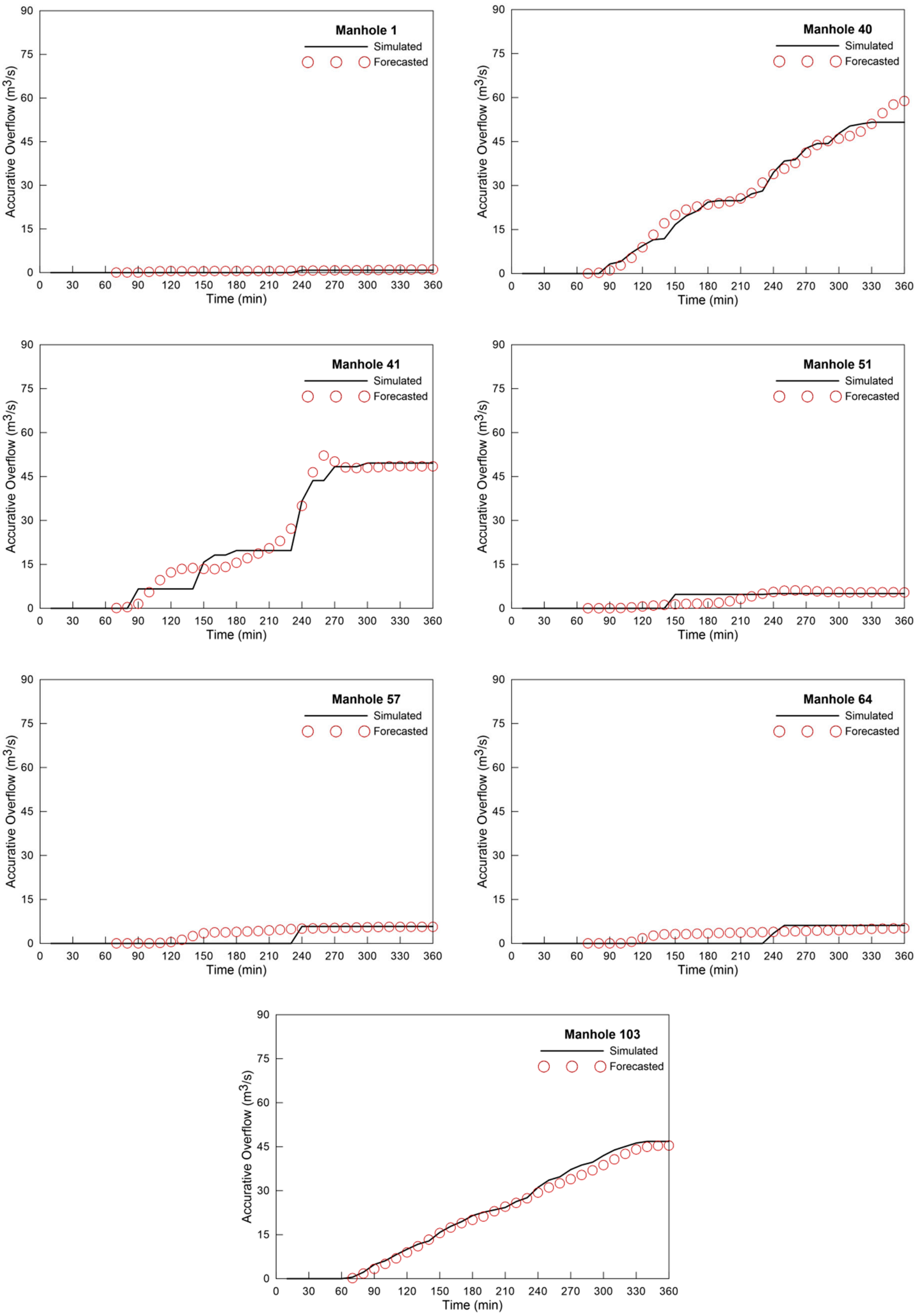

Figure 5. Accumulative overflow prediction results.

Table 2. Root mean square error (RMSE) at each manhole (21 September 2010 event).

Classification		Root Mean Square Error (m^3/s) at Each Manhole						
		Manhole 1	Manhole 40	Manhole 41	Manhole 51	Manhole 57	Manhole 64	Manhole 103
Time delay	T + 1	0.606	2.44	4.702	1.008	2.992	4.626	1.134
	T + 3	0.270	3.491	4.131	0.628	1.677	2.471	1.013
	T + 6	0.285	3.918	3.157	1.375	1.945	2.059	1.532

RMSE observations standard deviation ratio (RSR) was also considered for more statistical error analysis. RSR standardizes RMSE using the standard deviation in the observations, and it combines both an error index and some additional information. RSR was calculated as the ratio of the RMSE to the standard deviation of the measured data, as shown in Equation (2).

$$\mathrm{RSR} = \frac{\sqrt{\sum\left(Q_{\mathrm{simulated}} - Q_{\mathrm{predicted}}\right)^2}}{\sqrt{\sum\left(Q_{\mathrm{simulated}} - Q_{\mathrm{simulated.mean}}\right)^2}} \tag{2}$$

The coefficient of determination (R^2) was analyzed in addition to quantitative error analysis. The coefficient of determination is a square value of the correlation coefficient (R) and ranges from $0 \leq R^2 \leq 1$. This indicates that the simulated and predicted values have some constant tendencies, but the two values are not identical.

The Nash–Sutcliffe efficiency coefficient (NSEC) was used to evaluate the prediction performance of the model presented in this paper. The NSEC is a standardized value of residual relative degree that ranges from $-\infty < \mathrm{NSEC} \leq 1$. The closer the NSEC value is to 1, the more it indicates an accurate result of the prediction model. In Equations (1)–(3), $Q_{\mathrm{simulated}}$ refers to the simulated flow result, $Q_{\mathrm{predicted}}$ refers to the predicted flow result, and $\overline{Q}_{\mathrm{predicted}}$ refers to the mean of the predicted flow result. The values of RSR, NSEC, and R-square are represented in Table 3.

$$\mathrm{NSEC} = 1 - \frac{\sum\left(Q_{\mathrm{simulated}} - Q_{\mathrm{predicted}}\right)^2}{\sum\left(Q_{\mathrm{simulated}} - \overline{Q}_{\mathrm{predicted}}\right)^2} \tag{3}$$

Table 3. Total overflow error analysis.

Classification	RSR			Nash–Sutcliffe			R-Square		
	T + 1	T + 3	T + 6	T + 1	T + 3	T + 6	T + 1	T + 3	T + 6
Time delay	0.199	0.129	0.151	0.963	0.985	0.979	0.969	0.985	0.982

Accumulative overflow prediction results confirmed that, when compared to the results of error by delay time analysis, the longer the predicted delay time, the better the prediction ability. In the case of two-dimensional interpretation through predicted accumulative overflow, a 60 min prediction result delay time was used as well as LiDAR's detailed topographical data and composite roughness coefficient. Two-dimensional interpretation was conducted using the established topographical data and predicted overflow data, and a 10 min simulation of the 21 September 2010 rainfall event with 6 h duration was conducted. The process involved is shown in Figure 6.

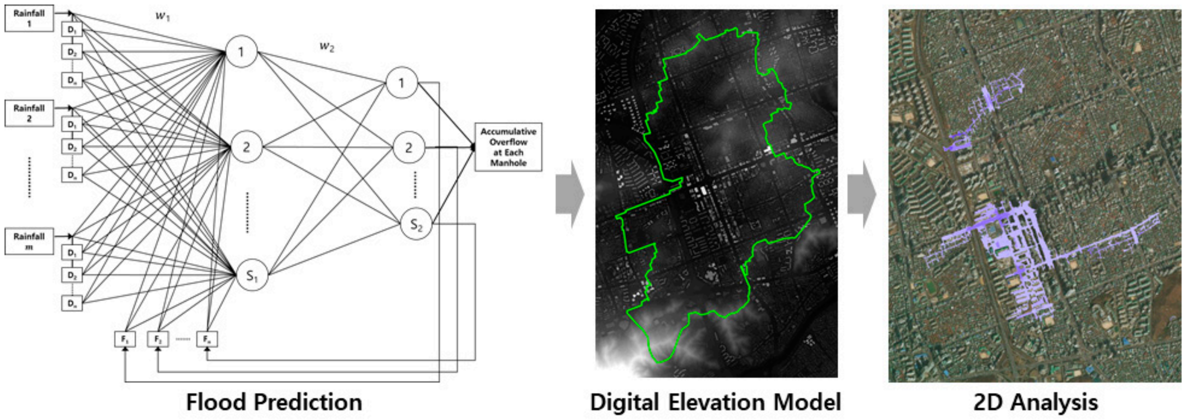

Figure 6. Flood prediction-based inundation map.

The results of conducting two-dimensional interpretation based on accumulative overflow prediction results are given in Figure 7, and the prediction result appropriateness was validated through the National Disaster Management System (NDMS) and inundation trace map. The suitability of the simulation results and the flooding trace was found to be 81%. Therefore, the inundation simulation results applied in this study were deemed to be feasible for application as baseline data for selecting evacuation routes by recurrence hour and evacuation center.

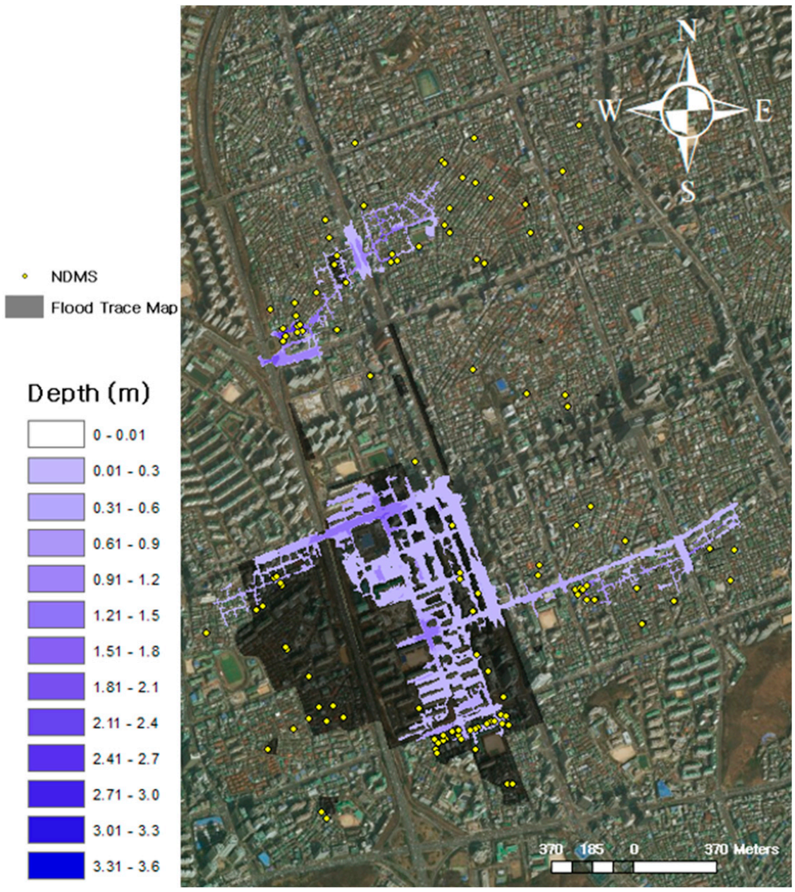

Figure 7. Inundation map results.

3.3. Spatial and Temporal Flood Hazard Analysis

Studies aiming to estimate the scale of damage loss arising from flooding have been carried out comprehensively, including such approaches as the development of the mortality rate function (e.g., [28,29]). However, studies of evacuation under life-threatening circumstances caused by floods are rare [30–33]. Studies of the direct and indirect effect of flooding on people have focused primarily on the inundation depth and velocity for evacuation by walking [25] (Table 4).

Table 4. Hazards as a function of inundation depth and velocity [25].

$d \times (v + 0.5)$	Flood Hazard Degree	Description
<0.75	Low	Caution "Flood zone with shallow flowing water or deep standing water"
0.75–1.25	Moderate	Dangerous for some (i.e., children) "Danger: flood zone with deep or fast flowing water"
1.25–2.5	Significant	Dangerous for most people "Danger: flood zone with deep fast flowing water"
>2.5	Extreme	Dangerous for all "Extreme danger: flood zone with deep fast flowing water"

DEFRA and the Environment Agency [25] mentioned the need for the classification of flood hazards and proposed a classification of inundation hazards that can be seen in Table 4. Otherwise, research into evacuation speed during inundation or risk classification have been carried out in preceding studies such as Kang [20], OFAT et al. [30], Ishigaki [31], Ishigaki et al. [32], and Lee et al. [34]. In this study, DEFRA and the Environment Agency's [25] risk classification method was applied based on inundation depth per hourly progress and velocity of flow via artificial neural network, and the flood hazard result obtained is shown in Figure 8 below. This method makes it easy to evaluate flood hazards based on the depth and flow velocity of the two-dimensional flood analysis and NARX results. Other previous research results mentioned above can provide data for categorizing flood hazards, but it is difficult to generalize because there are few test subjects, and experiments are conducted at characteristic places.

After 1 h, only a small district was flooded and there were no regions that exceeded 0.75 in terms of risk classification. However, after 2 h, there were some regions that exceeded a risk classification of 0.75. As can be seen in Table 5, regions with inundation risk increased rapidly between 1~2 h and 2~3 h.

Table 5. Time-dependent changes in flood hazard area.

Classification	1 h	2 h	3 h	4 h	5 h	6 h	7 h	8 h
Area (m^2)	0	71,625	150,600	150,825	150,925	151,475	151,575	151,750
Increment (m^2)	-	71,625	78,975	225	100	550	100	175

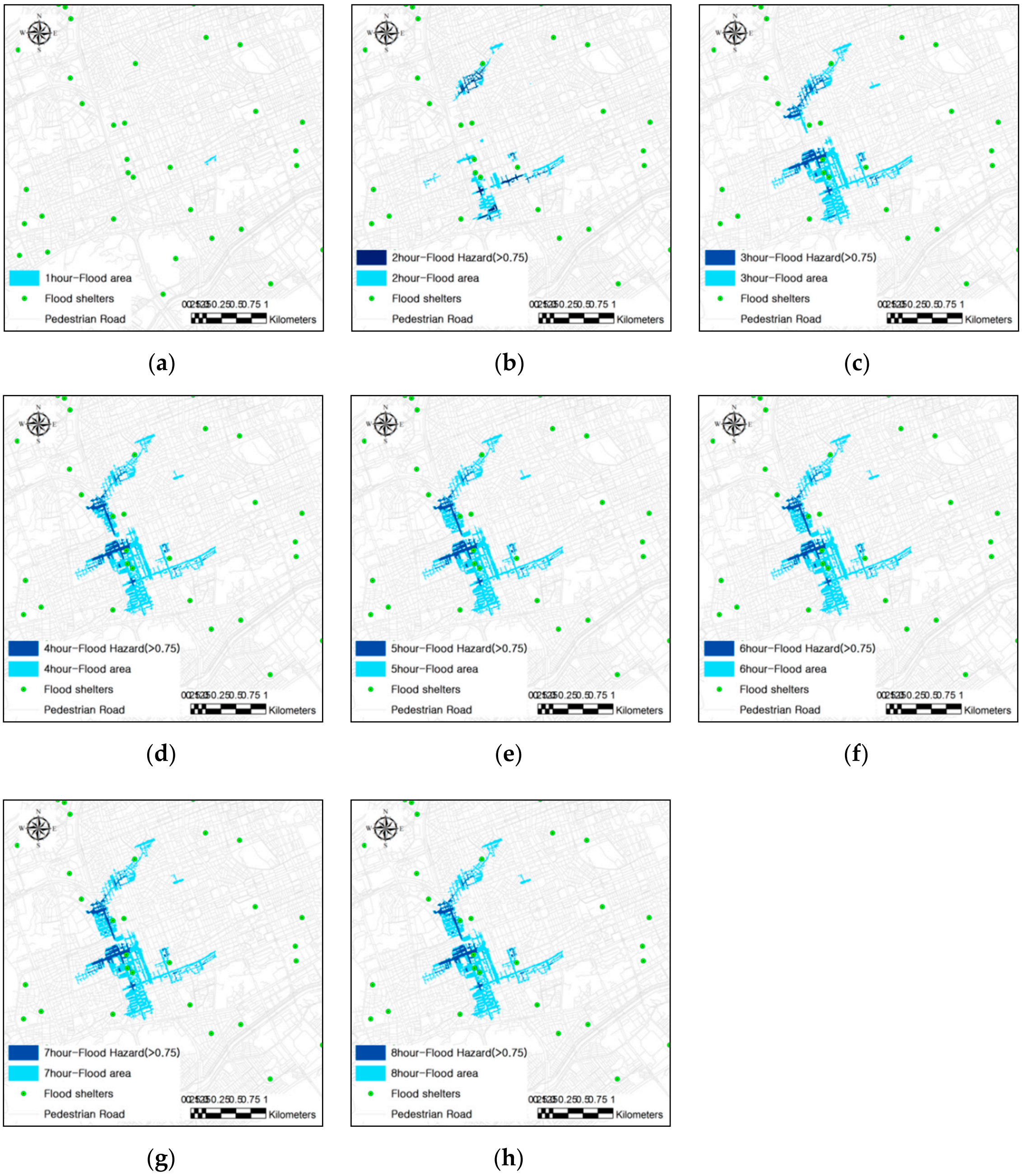

Figure 8. Flood hazard spatial and temporal variation analysis results (1~8 h). (**a**) 1 h elapsed; (**b**) 2 h elapsed; (**c**) 3 h elapsed; (**d**) 4 h elapsed; (**e**) 5 h elapsed; (**f**) 6 h elapsed; (**g**) 7 h elapsed; (**h**) 8 h elapsed.

3.4. Evacuation Route Analysis

In order to designate an evacuation route, there must be a point of departure and a destination. In this study, a building within the maximum expected flood scope was set as the demand point. The destination was the flood evacuation facility designated within the subject site. The area of maximum expected flood scope in the study area, Gangnam station region, is 772,425 m^2, and 1153 buildings are distributed within the expected scope. Location–allocation analyses have been utilized to establish evacuation plans, including evacuation routes in multiple preceding studies, but this study excluded quantitative analysis of evacuation demand and evacuation facility capacity.

Furthermore, as the assumption was made that evacuees would evacuate to the closest evacuation facility, the closest facility analysis was utilized to assign the evacuation route. In addition, prohibited pedestrian sector by hourly progress was set by overlapping flood risk regions identified in Section 3.3

with road data, and was utilized as a barrier of network analysis. The results of the evacuation route temporal and spatial variable analysis are given in Figure 9.

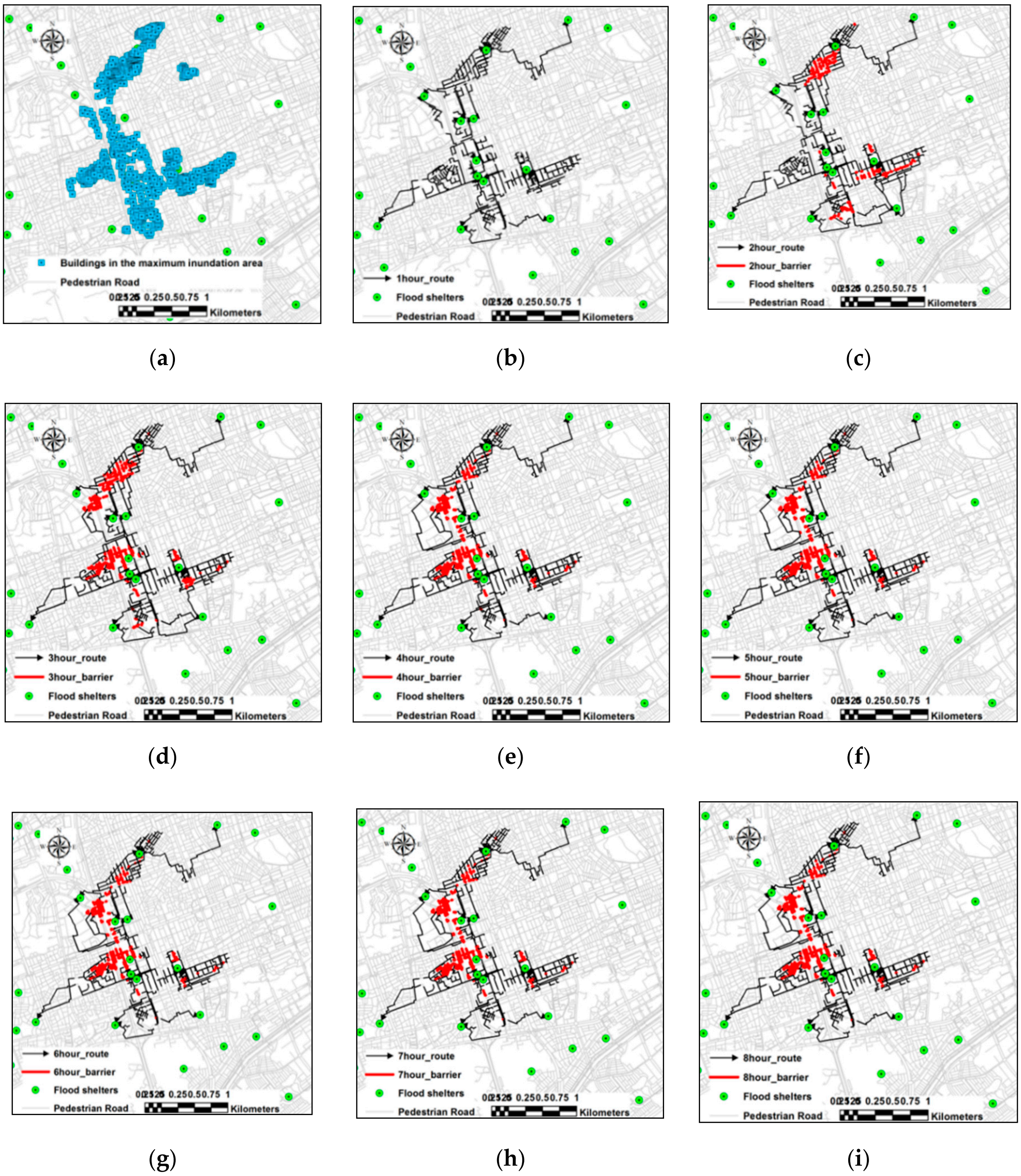

Figure 9. Evacuation route spatial and temporal variation analysis results (1~8 h). (**a**) Buildings in areas where flooding is expected; (**b**) 1 h elapsed; (**c**) 2 h elapsed; (**d**) 3 h elapsed; (**e**) 4 h elapsed; (**f**) 5 h elapsed; (**g**) 6 h elapsed; (**h**) 7 h elapsed; (**i**) 8 h elapsed.

In the event that evacuation is not carried out prior to flooding, the pedestrian evacuation hazard region increases with the inundation progress, and the number of buildings from which evacuation by walking was deemed impossible (dangerous) is shown in Table 6 below. After 2 h, 200 of the 1153 buildings distributed within the maximum inundation scope were deemed dangerous for evacuation by walking. The time when buildings would be predicted to have the highest ratio of evacuation by walking danger would be after 3 h (22.12%). Results further indicated that an average of 15.51% of buildings would be expected to face difficulty in terms of evacuation by walking.

Table 6. Analysis results for buildings with possibility of evacuation by walking by hourly progress.

Classification	Number of Buildings in Flooded Areas		
	Buildings Where Evacuation by Walking is Possible (a)	Buildings Where Evacuation by Walking not Possible (b)	Percentage of Buildings Where Evacuation by Walking not Possible (b/a + b)
1 h	1153	0	0.00%
2 h	953	200	17.35%
3 h	898	255	22.12%
4 h	957	196	17.00%
5 h	958	195	16.91%
6 h	958	195	16.91%
7 h	958	195	16.91%
8 h	958	195	16.91%

Analyzing the evacuation route under the assumption that evacuation by walking would cause a detour into dangerous regions, leading to the closest evacuation facility, the evacuation by walking distance by hourly progress results are shown in Figure 10 below. Buildings where evacuation by walking is impossible have been excluded from the evacuation by walking distance analysis in Table 6. Prior to flooding, the average evacuation distance from 1153 buildings to the closest evacuation facility was 478.85 m, and the longest evacuation distance was 1183.30 m. In the event of evacuation by avoiding regions where evacuation by walking is impossible (dangerous) as flooding progresses, it was determined that there would not be a significant change in the average walking distance by hourly progress.

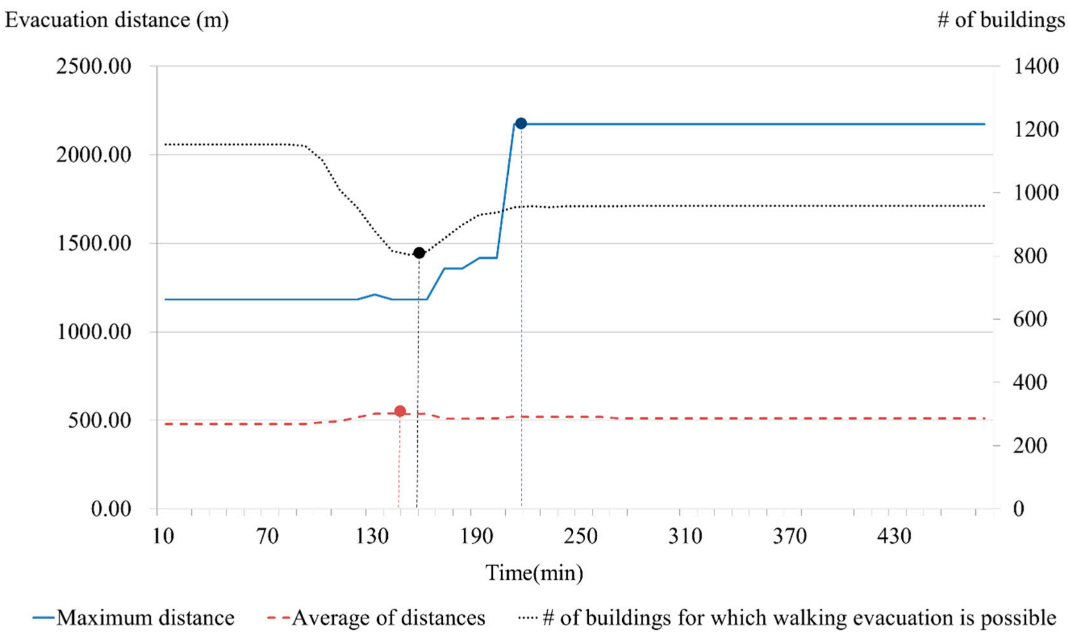

Figure 10. Time-dependent changes in pedestrian evacuation distance and number of buildings in the flooded area for which evacuation by walking is possible.

However, analysis indicated that the longest evacuation distance would increase significantly after 2 ~ 4 h, and that the occurrence of evacuation by walking hazard region (inundated buildings) following inundation progress increased rapidly between 90 ~ 160 min, and then dropped slightly.

Accordingly, the average evacuation by walking distance reached its maximum value at 140 min, but the maximum evacuation by walking distance occurred at 210 min. The number of buildings where evacuation by walking was impossible following evacuation by walking hazard region reached a maximum at 150 min.

4. Discussion

4.1. Inundation Forecasting

The purpose of this study was to identify an evacuation route with consideration of spatial inundation progress following the time lapse related to flooding after heavy rainfall. Moreover, inundation progress was predicted by using a dynamic artificial neural network because, ultimately, the aim was to provide a real-time evacuation route. This is because urban flood predictions based on numerical analysis models provide accurate and precise results, but the necessary pre- and post-processing takes quite some time. The accumulative overflow for manhole points was predicted through use of the NARX neural network, and after conducting two-dimensional inundation interpretation with the predicted value, an inundation map by hour was created. Comparing the inundation trace map and the NDMS resident report point concerning the two-dimensional interpretation results, appropriateness was judged to be 81%. By predicting the two-dimensional model input data with the NARX neural network, it was possible to save time following one-dimensional urban runoff interpretation. In this study, the inundation prediction via NARX neural network was completed within 3 s, and in the same computer environment, an inundation prediction via SWMM takes approximately 10 min. It can be applied to other river basins or stream floods if rainfall, flood data, and a spatial distribution technique of flood depth are provided. The rainfall, flood volume, and flood depth data can be calculated through a numerical analysis model or can be obtained from observed values. In this study, the flood depth was predicted through a flood volume prediction system using NARX and by linking a two-dimensional flood analysis model. It can be applied to other water basins or flood types if the data can be pre-processed sufficiently.

In this study, the total flood volume of the rainfall input data was predicted in real-time using the NARX neural network. This was then inputted into a two-dimensional flood analysis program to calculate the flood map. It is different from other studies that predict the flood volume only for rainfall events. Also, it has an advantage in that the predicted total flood volume is the sum of the flood volumes predicted for each of the manhole points and so the flood risk for each point can be identified quickly. Since the time may be depicted in the two-dimensional flood analysis simulation, if the spatial distribution of the flood depth can be predicted in real-time, it could be a very practical method. However, for the preparation of a two-dimensional inundation map in this study, the real-time provision of evacuation route information via numerical analysis was still poor.

4.2. Flood Hazard and Walking Evacuation

An evacuation route was selected under the assumption that buildings distributed within the maximum inundation scope were set as representing evacuation demand, and that people would evacuate to the closest evacuation facility. In the case of the study area, it was observed that buildings where evacuation by walking became impossible following inundation progress increased significantly after 2 ~ 3 h. Regarding the detour evacuation route distance, it was observed that this increased significantly after 2 ~ 4 h. Such analysis results show that adaptability and safety have to be ensured in inundated situations by planning in a flexible manner following the occurrence and change of evacuation by walking hazard regions in the process of selecting an evacuation route. Considering such results, the methodology of this study has been deemed usable for the purposes of establishing an evacuation plan that takes into account the situation after a disaster occurs. Although it can serve to contribute to the achievement of substantiation when establishing evacuation plans in the future, integrated analysis of occurrence and change in the evacuation by walking hazard region, distribution of buildings within the expected inundation region (evacuation demander), and the road network is required for this. Moreover, as 10 min and 1 h inundation prediction data were utilized to assign evacuation routes by hour in this study, the inundation progress of each point was not analyzed in detail. Therefore, it is recommended that studies such as the development of a methodology for evaluating the flood risk of pedestrian evacuation in a road network by analyzing the flooding progress in detail (e.g., trend analysis and space–time cluster analysis) be conducted. Such a methodology could lead to the development of an evacuation decision model for buildings in the expected flooding area according to the progress of flooding.

The flood hazard classification method applied in this study [25] can be applied to various flood types such as flash floods, coastal floods, and urban floods because it uses the relationship between flood depth and flow velocity. However, studies based on experiments [20,31,32,34] suggest that the inundation depth of a specific location (e.g., underground or stairs) or water level that an adult can walk in is 30 ~ 50 cm. Therefore, careful notice must be taken when applying the flood hazard risk classification of DEFRA and the Environment Agency [25]. Also, it is necessary to modify the standards related to flood hazard to people through the collection of experimental data related to the safety of people during a flood according to the specific location or their gender, age, and disability.

Evacuees often choose the wrong direction (due to personal wrong choice or leader follow effect) due to panic or lack of evacuation information. To prevent this, it is important to provide real-time evacuation information to evacuees. In this respect, real-time evacuation guidance using mobile applications is drawing attention from researchers (e.g., [35–37]). By applying the methodology proposed in this study, it is possible to minimize the casualties caused during the evacuation process by selecting the evacuation route when flooding occurs. However, for real-time evacuation guidance, the role of IoT (Internet of Things) technologies is important because it is necessary to provide the evacuee's location-based evacuation routes. Evacuation guidance and information related to IoT technologies have recently attracted the attention of researchers and have been studied by Krytska et al. [38], Zualkernan et al. [39], and Yin et al. [40], for example.

Meanwhile, "in rapid-onset disasters the time needed for evacuation is crucial" [41]. However, in large-scale evacuation situations, time delays occur due to congestion (e.g., bottleneck effect). Phased evacuation was suggested in a simulation-based previous study [42–44] as a method to reduce the time delay due to congestion in an evacuation situation. Since this study focuses on the prediction of the changing pattern of urban flooding according to the progress of flooding, it can be used to establish a phased evacuation strategy.

5. Conclusions

This study aimed to perform inundation map forecasting with artificial neural network-based methodology. In addition, it proposed a methodology for selecting an evacuation route by considering temporal and spatial evacuation by walking hazard. Previous studies have not focused on the necessity of temporal and spatial changes in the flood evacuation route, but this study once again demonstrates that need. In addition, the evacuation route is determined according to the hazard of walking evacuation, thus minimizing the hazard for evacuees during the evacuation process. The proposed methodology is not a field test-based or practical application method for establishing a flood evacuation plan, but it shows great potential in terms of efficiency. For example, if a further study can predict not only urban runoff but also inundation map, the evacuation route can be calculated more quickly. In addition, the proposed methodology can be extended to a model for calculating the spatial and temporal changes in evacuation demand according to the flooding progress. It is envisaged that this research will provide a basis for future comprehensive and cohesive research on flood evacuation strategies according to the progress of flooding. In turn, research will lead to better preparedness and response to flood evacuation problems.

Author Contributions: All authors contributed extensively to the work. Y.H.L. and W.H.H. conceptualized and designed the study. Y.H.L. and H.I.K. produced the data required to apply the methodology to the study area and

conducted the model simulation, validation, and writing—original draft preparation. Y.H.L. and H.I.K. analyzed the results, completed the manuscript, wrote the review, and conducted editing. K.Y.H. and W.H.H. supervised the project and acquired the funding. All authors have read and agreed to the published version of the manuscript.

Funding: This research was funded by the Korea Ministry of Environment (MOE).

Acknowledgments: This work was supported by the Korea Environment Industry & Technology Institute (KEITI) though the Water Management Research Program, funded by the Korea Ministry of Environment (MOE) (79609).

Conflicts of Interest: The authors declare no conflict of interest.

References

1. Liu, X.; Lim, S. A Spatial Analysis Approach to Evacuation Management: Shelter Assignment and Routing; Research@Locate'15, Brisbane, Australia. 10–12 March 2015. Available online: http://ceur-ws.org (accessed on 23 July 2020).
2. Hwang, K.; Schuetze, T.; Amoruso, F.M. Flood Resilient and Sustainable Urban Regeneration Using the Example of an Industrial Compound Conversion in Seoul, South Korea. *Sustainability* **2020**, *12*, 918. [CrossRef]
3. Jha, A.K.; Bloch, R.; Lamond, J. *Cities and Flooding: A Guide to Integrated Urban Flood Risk Management for the 21st Century*; The World Bank: Washington, DC, USA, 2012.
4. Atmojo, P.S.; Sachro, S.S. Disaster management: Selections of evacuation routes due to flood disaster. *Procedia Eng.* **2017**, *171*, 1478–1485. [CrossRef]
5. Lee, B. A study on the characteristics and composition direction of urban flood control system. *Water Future* **2006**, *39*, 50–54.
6. Kim, J.; Kuwahara, Y.; Kumar, M. A DEM-based evaluation of potential flood risk to enhance decision support system for safe evacuation. *Nat. Hazards* **2011**, *59*, 1561–1572. [CrossRef]
7. Kim, H.I.; Keum, H.J.; Han, K.Y. Real-Time Urban Inundation Prediction Combining Hydraulic and Probabilistic Methods. *Water* **2019**, *11*, 293. [CrossRef]
8. Mosavi, A.; Ozturk, P.; Chau, K.W. Flood Prediction Using Machine Learning Models: Literature Review. *Water* **2018**, *10*, 11. [CrossRef]
9. Jhong, B.; Wang, J.; Lin, G. Improving the long lead-time inundation forecasts using effective typhoon characteristics. *Water Resour. Manag.* **2016**, *30*, 4247–4271. [CrossRef]
10. Granata, F.; Gargano, R.; De Marinis, G. Support vector regression for rainfall-runoff modeling in urban drainage: A comparison with the EPA's storm water management model. *Water* **2016**, *8*, 69. [CrossRef]
11. Tehrany, M.S.; Pradhan, B.; Mansor, S.; Ahmad, N. Flood Susceptibility Assessment Using GIS-based Support Vector Machine Model with Different Kernel Types. *Catena* **2015**, *125*, 91–101. [CrossRef]
12. Chang, L.; Amin, M.Z.M.; Yang, S.; Chang, F. Building ANN-based regional multi-step-ahead flood inundation forecast models. *Water* **2018**, *10*, 1283. [CrossRef]
13. Zhou, J.; Peng, T.; Zhang, C.; Sun, N. Data pre-analysis and ensemble of various artificial neural networks for monthly streamflow forecasting. *Water* **2018**, *10*, 628. [CrossRef]
14. Hu, C.; Wu, Q.; Li, H.; Jian, S.; Li, N.; Lou, Z. Deep learning with a long short-term memory networks approach for rainfall-runoff simulation. *Water* **2018**, *10*, 1543. [CrossRef]
15. Rahman, M.; Ningsheng, C.; Islam, M.M.; Dewan, A.; Iqbal, J.; Washakh, R.M.A.; Shufeng, T. Flood Susceptibility Assessment in Bangladesh Using Machine Learning and Multi-criteria Decision Analysis. *Earth Syst. Environ.* **2019**, *3*, 585–601. [CrossRef]
16. Na, L.; Xueyan, S.; Mingliang, Q. A bi-objective evacuation routing engineering model with secondary evacuation expected costs. *Syst. Eng. Procedia* **2012**, *5*, 1–7. [CrossRef]
17. Lim, H., Jr.; Lim, M.B.; Piantanakulchai, M. A review of recent studies on flood evacuation planning. *J. East. Asia Soc. Transp. Stud.* **2013**, *10*, 147–162.
18. Shekhar, S.; Yang, K.; Gunturi, V.M.; Manikonda, L.; Oliver, D.; Zhou, X.; George, B.; Kim, S.; Wolff, J.M.; Lu, Q. Experiences with evacuation route planning algorithms. *Int. J. Geogr. Inf. Sci.* **2012**, *26*, 2253–2265. [CrossRef]
19. Mayunga, J.S. Assessment of public shelter user's satisfaction: Lessons learned from south-central Texas flood. *Nat. Hazards Rev.* **2012**, *13*, 82–87. [CrossRef]
20. Kang, S. Study on refuge behavior and its critical inundation depth in low area. *J. Korean Soc. Civ. Eng.* **2003**, *23*, 561–565.

21. Arabani, A.B.; Farahani, R.Z. Facility location dynamics: An overview of classifications and applications. *Comput. Ind. Eng.* **2012**, *62*, 408–420. [CrossRef]
22. Ahmad, S.S.; Simonovic, S.P. Spatial and temporal analysis of urban flood risk assessment. *Urban Water J.* **2013**, *10*, 26–49. [CrossRef]
23. Huang, H.; Chen, X.; Zhu, Z.; Xie, Y.; Liu, L.; Wang, X.; Wang, X.; Liu, K. The changing pattern of urban flooding in Guangzhou, China. *Sci. Total Environ.* **2018**, *622*, 394–401. [CrossRef] [PubMed]
24. Chen, H.; Ito, Y.; Sawamukai, M.; Su, T.; Tokunaga, T. Spatial and temporal changes in flood hazard potential at coastal lowland area: A case study in the Kujukuri Plain, Japan. *Nat. Hazards* **2016**, *84*, 1513–1527. [CrossRef]
25. DEFRA and the Environment Agency. *R&D Outputs: Flood Risks to People. Phase 2. FD2321/TR1 The Flood Risks to People Methodology*; Department for Environment Food and Rural Affairs and the Environment Agency: London, UK, 2006.
26. Choi, S.; Yoon, S.; Lee, B.; Choi, Y. Evaluation of high-resolution QPE data for urban runoff analysis. *J. Korea Water Resour. Assoc.* **2015**, *48*, 719–728. [CrossRef]
27. Shen, H.; Chang, L. Online multistep-ahead inundation depth forecasts by recurrent NARX networks. *Hydrol. Earth Syst. Sci.* **2013**, *17*, 935. [CrossRef]
28. Penning-Rowsell, E.; Floyd, P.; Ramsbottom, D.; Surendran, S. Estimating injury and loss of life in floods: A deterministic framework. *Nat. Hazards* **2005**, *36*, 43–64. [CrossRef]
29. Jonkman, S.; Vrijling, J.; Vrouwenvelder, A. Methods for the estimation of loss of life due to floods: A literature review and a proposal for a new method. *Nat. Hazards* **2008**, *46*, 353–389. [CrossRef]
30. OFEE, OFAT, OFEFP, 1997: Prise en Compte des Dangers dus aux Crues dans le Cadre des Activités de l'Aménagement du Territoire. Recommandations, Office Fédéral de l'Économie des Eaux (OFEE), Office Fédéral de l'Aménagement du Territoire (OFAT), Office fédéral de l'Environnement, des Forêts et du Paysage (OFEFP). Available online: http://www.planat.ch/fileadmin/PLANAT/planat_pdf/alle_2012/1996-2000/Lateltin_1997_-_Prise_en_compte_des_dangers.pdf (accessed on 23 March 2020).
31. Ishigaki, T. Evacuation criteria during urban flooding in underground space. In Proceedings of the 11th ICUD, Edinburgh, UK, 31 August–5 September 2008.
32. Ishigaki, T.; Baba, Y.; Toda, K.; Inoue, K. Experimental study on evacuation from underground space in urban flood. In Proceedings of the Korea Water Resources Association Conference, Iksan, Korea, 20–21 May 2005; pp. 261–262.
33. Jonkman, S.; Penning-Rowsell, E. Human Instability in Flood Flows 1. *JAWRA J. Am. Water Resour. Assoc.* **2008**, *44*, 1208–1218. [CrossRef]
34. Lee, H.; Hong, W.; Lee, Y. Experimental study on the influence of water depth on the evacuation speed of elderly people in flood conditions. *Int. J. Disaster Risk Reduct.* **2019**, *39*, 101198. [CrossRef]
35. Zhang, P.; Liu, Y.; Yang, R.; Zhang, H.; Gong, Z. Improving urban traffic evacuation capability in emergency response by using smart phones. In Proceedings of the Asia-Pacific Web Conference, Suzhou, China, 23–25 September 2016; Springer: Cham, Switzerland, 2016; pp. 241–252.
36. Kairupan, I.; Huang, Z.Y.; Chang, H.C.; Chang, C.W. Emergency navigation and alarm with flooding models—A real case study of Manado City. In Proceedings of the 2016 International Conference on Communication Problem-Solving (ICCP), Taipei, Taiwan, 7–9 September 2016; pp. 1–2.
37. Krajewski, W.F.; Ceynar, D.; Demir, I.; Goska, R.; Kruger, A.; Langel, C.; Mantilla, R.; Niemeier, J.; Quintero, F.; Seo, B.C.; et al. Real-time flood forecasting and information system for the state of Iowa. *Bull. Am. Meteorol. Soc.* **2017**, *98*, 539–554. [CrossRef]
38. Krytska, Y.; Skarga-Bandurova, I.; Velykzhanin, A. IoT-based situation awareness support system for real-time emergency management. In Proceedings of the 9th IEEE International Conference on Intelligent Data Acquisition and Advanced Computing Systems: Technology and Applications (IDAACS), Bucharest, Romania, 21–23 September 2017; Volume 2, pp. 955–960.
39. Zualkernan, I.A.; Aloul, F.A.; Sakkia, V.; Al Noman, H.; Sowdagar, S.; Al Hammadi, O. An IoT-based Emergency Evacuation System. In Proceedings of the IEEE International Conference on Internet of Things and Intelligence System (IoTaIS), Bali, Indonesia, 5–7 November 2019; pp. 62–66.
40. Yin, L.; Chen, J.; Zhang, H.; Yang, Z.; Wan, Q.; Ning, L.; Hu, J.; Yu, Q. Improving emergency evacuation planning with mobile phone location data. *Environ. Plan. B Urban. Anal. City Sci.* **2020**, *47*, 964–980. [CrossRef]

41. Kubisch, S.; Stötzer, J.; Keller, S.; Bull, M.T.; Braun, A. Combining a social science approach and GIS-based simulation to analyse evacuation in natural disasters: A case study in the Chilean community of Talcahuano. In Proceedings of the 16th International Conference on Information Systems for Crisis Response and Management (ISCRAM 2019), Valencia, Spain, 19–22 May 2019.
42. Li, M.; Xu, J.; Li, J.; Liu, X.; Ru, H.; Sun, C. A model for phased evacuations for disasters with spatio-temporal randomness. *Int. J. Geogr. Inf. Sci.* **2019**, *33*, 922–944. [CrossRef]
43. Zhang, Z.; Spansel, K.; Wolshon, B. Effect of phased evacuations in megaregion highway networks. *Transp. Res. Rec. J. Transp. Res. Board* **2014**, *2459*, 101–109. [CrossRef]
44. O'Shea, T.; Bates, P.; Neal, J. An agent-based model for flood risk warning. *Nat. Hazards Earth Syst. Sci. Discuss.* **2019**, 1–32. [CrossRef]